VOLUME 123, NUMBER 11
MARCH 21, 2001

JOURNAL OF THE AMERICAN CHEMICAL SOCIETY

Recognition of Nine Base Pairs in the Minor Groove of DNA by a Tripyrrole Peptide−Hoechst Conjugate

Alexander L. Satz and Thomas C. Bruice*

Contribution from the Department of Chemistry and Biochemistry, University of California at Santa Barbara, Santa Barbara, California 93106

Received August 21, 2000

Abstract: A tripyrrole peptide−Hoechst conjugate (FPH-1) has been designed which recognizes nine dA/dT base pair A/T rich dsDNA sequences at subnanomolar concentrations and complexes its targets at near diffusion controlled rates to form a fluorescent product. Spectrofluorometric titrations show the stoichiometry of the complex to be $(FPH\text{-}1)_2$:dsDNA. Spectrofluorometric titrations were also employed to determine the product of the equilibrium constant for complexation (K_1K_2) of dsDNA by two FPH-1 molecules for 35 different oligomeric duplexes. Single base pair mismatches in the FPH-1 binding site were found to cause significant decreases in K_1K_2 of 18- to 2300-fold. Thermal denaturation experiments provided similar results. Arguments are presented which favor the structure of the $(FPH\text{-}1)_2$:dsDNA minor groove complex to involve the two FPH-1 molecules in a slightly staggered, side-by-side, and antiparallel arrangement such that the bis-benzimidazole moiety of one FPH-1 molecule lies adjacent to the tripyrrole moiety of the second FPH-1 molecule.

Introduction

Organic compounds which bind the minor groove of B-DNA with sequence selective recognition have drawn considerable attention.[1−6] Studies indicate that these agents may influence the regulation of gene expression by inhibiting the binding of regulatory proteins to their DNA binding sites. [1,7−9] Interest in the control of expression of specific genes has spurred efforts in the development of new minor groove binding agents. It is expected that those capable of recognizing longer DNA sequences will exhibit the greatest specificity; however those few agents targeted to longer DNA sequences have generally lacked binding specificity.[10−19]

Minor groove binders such as Hoechst 33258 and tripyrrole

(1) Kielkopf, C. L.; Bremer, R. E.; White, S.; Szewczyk, J. W.; Turner, J. M.; Baird, E. E.; Dervan, P. B.; Rees, D. C. *J. Mol. Biol.* **2000**, *295*, 557−567.
(2) Sharma, S. K.; Tandon, M.; Lown, J. W. *J. Org. Chem.* **2000**, *65*, 1102−1107.
(3) Xuereb, H.; Maletic, M.; Gildersleeve, J.; Pelczer, I.; Kahne, D. *J. Am. Chem. Soc.* **2000**, *122*, 1883−1890.
(4) Zimmer, C.; Wähnert, U. *Prog. Biophys. Mol. Biol.* **1986**, *47*, 31−112.
(5) Boger, D. L.; Johnson, D. S. *Angew. Chem., Int. Ed. Engl.* **1996**, *35*, 1438−1474.
(6) Bailly, C.; Chaires, J. B. *Bioconjugate Chem.* **1998**, *9*, 513−538.
(7) Gottesfeld, J. M.; Neely, L.; Trauger, J. W.; Baird, E. E.; Dervan, P. B. *Nature* **1997**, *387*, 202−205.
(8) Chiang, S. Y.; Bruice, T. C.; Azizkhan, J. C.; Gawron, L.; Beerman, T. A. *Proc. Natl. Acad. Sci. U.S.A.* **1997**, *94*, 2811−2816.
(9) Simon, H.; Kittler, L.; Baird, E.; Dervan, P.; Zimmer, C. *FEBS Lett.* **2000**, *471*, 173−176.
(10) Trauger, J. W.; Baird, E. E.; Dervan, P. B. *J. Am. Chem. Soc.* **1998**, *120*, 3534−3535.
(11) Kissinger, K. L.; Dabrowiak, J. C.; Lown, J. W. *Chem. Res. Toxicol.* **1990**, *3*, 162−168.
(12) Chen, Y. H.; Yang, Y. W.; Lown, J. W. *J. Biomol. Struct. Dyn.* **1996**, *14*, 341−355.
(13) Turner, J. M.; Baird, E. E.; Dervan, P. B. *J. Am. Chem. Soc.* **1997**, *119*, 7636−7644.
(14) Trauger, J. W.; Baird, E. E.; Mrksich, M.; Dervan, P. B. *J. Am. Chem. Soc.* **1996**, *118*, 6160−6166.

10.1021/ja003095d CCC: $20.00
Published on Web 02/17/2001

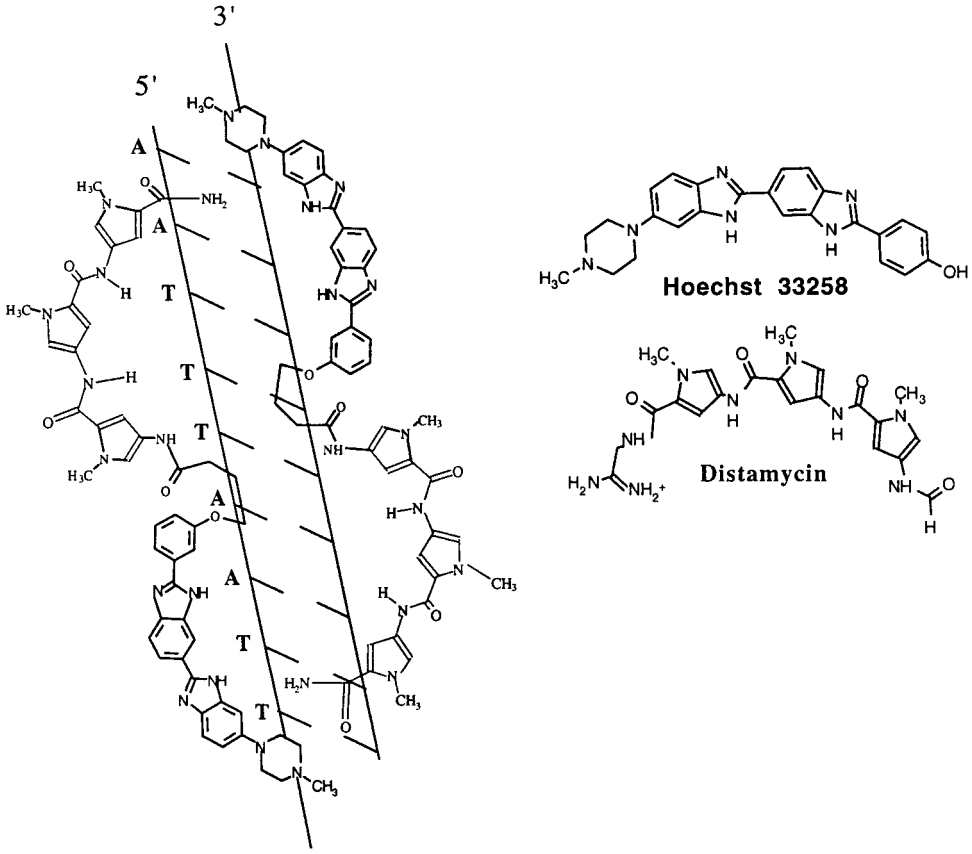

Figure 1. The chemical structures of $(FPH\text{-}1)_2$:dsDNA complex, Hoechst 33258, and distamycin.

peptides bind in the minor groove of dsDNA at runs of four or more A/T base pairs (Figure 1).[4] Regions of DNA that are unusually rich in A/T base pairs play key roles in the structure and function of the eukaryotic genome. This is partly attributable to the ability of AT-rich sequences to produce bent DNA or be readily unwound and unpaired in supercoiled DNA. Importantly, many nuclear proteins specifically recognize AT-rich DNA sequences, for example, mammalian HMGI protein and TATA-box binding protein TBP.[20]

We report here the study of a tripyrrole peptide−Hoechst conjugate (FPH-1) designed as a minor groove binding agent capable of recognizing nine base pair A/T rich DNA sequences (Figure 1). FPH-1 is fluorescent when bound in the minor groove of dsDNA. The agent was designed, with the aid of molecular modeling, to bind DNA as a side-by-side staggered antiparallel dimer as depicted in Figures 2 and 3.[2,21,22] We have investigated the binding of FPH-1 and Hoechst 33258 to the 18 base pair double-stranded DNA oligomer 5′-GCGGTATAAAATTC-GACG-3′ (**1**) and the 17 base pair oligomer 5′-GCGAATT-TAATTCGACG-3′ (**12**). Oligomer **1** contains the TATA box, which in eukaryotes consists of the consensus sequence 5′-TATAAAA-3′, and is recognized by the TBP (TATA binding protein) subunit of TFIID of the RNA polymerase II transcription initiation complex.[23] Oligomer **12** demonstrates the effect of substituting adenine and thymine bases within the FPH-1 binding site. Interactions between FPH-1 and 18 different oligomeric duplexes containing single base pair mismatches of **1** and **12** were investigated to determine sequence selectivity. Also investigated are the effect of double base pair mismatches as contained within oligomeric duplexes **11** and **22**−**24** (Table 1). Last, kinetic investigations show FPH-1 to complex its dsDNA target at a near diffusion controlled rate.

Experimental Section

Materials. Purified DNA oligomers were purchased from the Biomolecular Resource Center, University of California at San Francisco. Hoechst 33258 and 0.05 wt % 3-(trimethylsilyl)propionic-*2,2,3,3-d*$_4$ acid, sodium salt in D_2O were purchased from Aldrich and used without further purification. Solvents, and most reagents including triisopropylsilane (TIS), trifluoroacetic acid (TFA), dichloromethane (DCM), dimethylformamide (DMF), dicyclohexylcarbodiimide (DCC), diisopropylethylamine (DIPEA), acetonitrile (ACN), and hydroxybenzotriazole (HOBt), were purchased from Aldrich Chemical Co. Some reagents used for solid-phase chemistry including Rink amide MBHA resin and PyBOP[24] were bought from Novabiochem. The synthesis of **34** has been previously published.[25]

Procedures (DNA Binding Experiments). Oligomeric duplexes were formed by annealing complementary oligomers by heating equal molar mixtures to 95 °C for 10 min and slowly cooling to ambient temperature. Molar extinction coefficients for oligomeric duplexes were

(15) Kelly, J. J.; Baird, E. E.; Dervan, P. B. *Proc. Natl. Acad. Sci. U.S.A.* **1996**, *93*, 6981−6985.
(16) Singh, M. P.; Plouvier, B.; Hill, G. C.; Gueck, J.; Pon, R. T.; Lown, J. W. *J. Am. Chem. Soc.* **1994**, *116*, 7006−7020.
(17) Beerman, T. A.; Woynarowski, J. M.; Sigmund, R. D.; Gawron, L. S.; Rao, K. E.; Lown, J. W. *Biochim. Biophys. Acta* **1991**, *1090*, 52−60.
(18) Filipowsky, M. E.; Kopka, M. L.; Brazilzison, M.; Lown, J. W.; Dickerson, R. E. *Biochemistry* **1996**, *35*, 15397−15410.
(19) Lown, J. W.; Krowicki, K.; Balzarini, J.; Newman, R. A.; Declercq, E. *J. Med. Chem.* **1989**, *32*, 2368−2375.
(20) Forde, B. G. *Plant promoters and transcription factors*; Nover, L., Ed.; Springer-Verlag: Berlin; New York, 1994; pp 87−103.
(21) Kopka, M. L.; Goodsell, D. S.; Han, G. W.; Chiu, T. K.; Lown, J. W.; Dickerson, R. E. *Structure* **1997**, *5*, 1033−1046.
(22) Wemmer, D. *Nat. Struct. Biol.* **1998**, *5*, 169−171.
(23) Latchman, D. S. *Gene regulation: a eukaryotic perspective*, 3rd ed.; Stanley Thornes: Cheltenham, 1998.
(24) Coste, J.; Lenguyen, D.; Castro, B. *Tetrahedron Lett.* **1990**, *31*, 205−208.
(25) Satz, A. L.; Bruice, T. C. *Bioorg. Med. Chem.* **2000**, *8*, 1871−1880.

Table 1. Product of Equilibrium Association Constants for Complexation ($K_1K_2 \times 10^{-14}$ M^{-2})

	FPH-1	Ht33258
A. 18 Base Pair dsDNA Oligomers[a,b]		
5′-GCGGTATAAAATTCGACG-3′ (**1**)	37 000	5200
5′-GCGG**C**ATAAAATTCGACG-3′ (**2**)	1400	
5′-GCGGT**G**TAAAATTCGACG-3′ (**3**)	940	
5′-GCGGTA**C**AAAATTCGACG-3′ (**4**)	900	
5′-GCGGTAT**G**AAATTCGACG-3′ (**5**)	2100	
5′-GCGGTATA**G**AATTCGACG-3′ (**6**)	16	1634
5′-GCGGTATAA**G**ATTCGACG-3′ (**7**)	1300	
5′-GCGGTATAAA**G**TTCGACG-3′ (**8**)	620	
5′-GCGGTATAAAA**C**TCGACG-3′ (**9**)	620	
5′-GCGGTATAAAAT**C**CGACG-3′ (**10**)	1300	
5′-GCGGTATA**GG**AATTCGCG-3′ (**11**)	2	3800
B. 17 Base Pair dsDNA Oligomers		
5′-GCGAATTTAATTCGACG-3′ (**12**)	225 000	3100
5′-GCG**G**ATTTAATTCGACG-3′ (**13**)	7500	
5′-GCGA**G**TTTAATTCGACG-3′ (**14**)	1800	
5′-GCGAA**C**TTAATTCGACG-3′ (**15**)	1900	
5′-GCGAAT**C**TAATTCGACG-3′ (**16**)	321	
5′-GCGAATT**C**AATTCGACG-3′ (**17**)	512	2500
5′-GCGAATTT**G**ATTCGACG-3′ (**18**)	400	
5′-GCGAATTTA**G**TTCGACG-3′ (**19**)	290	
5′-GCGAATTTAA**C**TCGACG-3′ (**20**)	150	
5′-GCGAATTTAAT**C**CGACG-3′ (**21**)	500	
5′-GCGAATT**CC**AATTGACG-3′ (**22**)	25	9200
5′-GCGA**C**TT**C**AATTCGACG-3′ (**23**)	31	
5′-GCG**G**ATT**G**AATTCGACG-3′ (**24**)	31	

[a] Determined by nonlinear least-squares fitting of an isothermal binding curve. Equilibrium constants are given as the product of K_1K_2 for 2:1 ligand:DNA stoichiometries since separation of the individual equilibrium constants is not possible. The stated equilibrium constants have a standard deviation of ±60%. [b] The FPH-1 binding site is underlined. Mismatch sites are typed in bold face.

approximated using $A_{260} = 16\,800$ M^{-1} (G/C base pair)$^{-1}$ and $A_{260} = 13\,600$ M^{-1} (A/T base pair)$^{-1}$. Solutions of known ligand concentrations were prepared via peak integration of the ligand's NMR spectra where the ligand samples used contained a known quantity of the internal standard 3-(trimethylsilyl)propionic-*2,2,3,3-d*$_4$ acid, sodium salt.[25] UV/vis spectra were acquired on a Cary 100 Bio UV−vis spectrophotometer equipped with a temperature programmable cell block. All thermal melting experiments were carried out using 10 mM potassium phosphate, 150 mM, pH 7.0 buffer. For each series of thermal melting curves acquired using a particular oligomeric duplex (for example, **1** + no ligand **1** + Ht33258 **1** + FPH-1), dsDNA concentrations were kept constant and 2 equiv of ligand was added. The dsDNA concentrations employed ranged from 0.25 to 0.42 μM. Data points were taken every 1 °C with a temperature ramp of 0.5 °C min^{-1}. Thermal melting temperatures were calculated by first-derivative analysis. Fluorescence spectra were obtained on a Perkin-Elmer LS50B fluorimeter equipped with a constant temperature water bath set at 26 °C. Solutions were excited at 345 nm. Emissions were monitored at 450 or 470 nm. Spectrofluorometric titrations were obtained by titrating a constant concentration of DNA, usually between 1 and 500 nM, with a relatively concentrated solution of ligand.

Following determination of ligand:dsDNA complex stoichiometries, equilibrium constants for dsDNA complexation were investigated by generating isothermal binding curves via spectrofluorometric titrations (titration of a dilute dsDNA solution with ligand). Equilibrium constants for 2:1 ligand:dsDNA stoichiometries were calculated by fitting isothermal binding curves using eqs 1 and 2 (Figure 5).[25] Equation 1 was employed to fit plots of fluorescence vs concentration of unbound ligand ($[L]_f$), where $[L]_f$ is calculated by eq 2. The derivation and use of eqs 1 and 2 have been discussed by our laboratory.[25,26] Table 1 lists the calculated equilibrium constants for complexation.

(26) Browne, K. A.; He, G. X.; Bruice, T. C. *J. Am. Chem. Soc.* **1993**, *115*, 7072−7079.

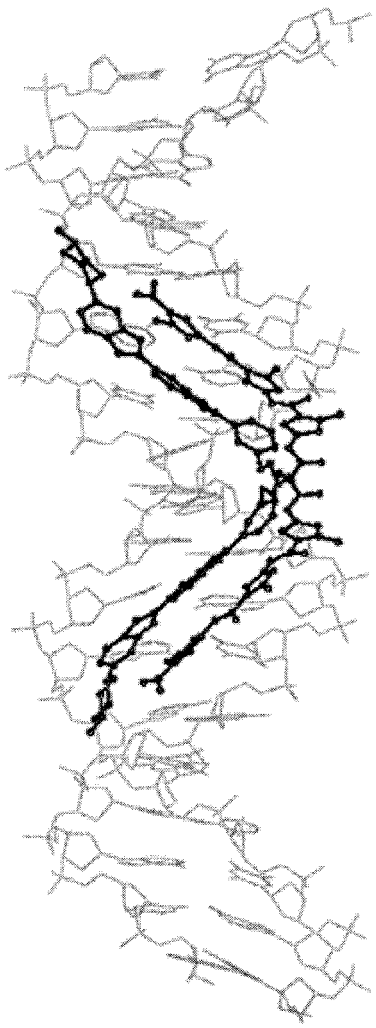

Figure 2. Computer-generated model of proposed $(FPH\text{-}1)_2$:dsDNA side-by-side antiparallel staggered complex.

$$F = \Sigma\Phi_f\left(\frac{0.5K_l[L]_f + K_1K_2[L]_f^2}{1 + K_1[L]_f + K_1K_2[L]_f^2}\right) \quad (1)$$

$$F = \Sigma\Phi_f\frac{[L]_{Bound}}{n[DNA]_T} \quad (2)$$

In eq 1 $\Sigma\Phi_f$ is the total fluorescence intensity upon saturation of dsDNA binding sites with ligand, K_1 and K_2 are the equilibrium association constants for the first and second binding events, and $[L]_f$ is the concentration of ligand free in solution. In eq 2 $[L]_{Bound}$ is the concentration of ligand bound to dsDNA, n is the stoichiometry of binding, and $[DNA]_T$ is the total concentration of duplex DNA in the sample.

For generation of meaningful isothermal binding curves, the general rule is that $[DNA]_T = 1/K_1$, where K_1 is the equilibrium constant for complexation of dsDNA in cases where the binding stoichiometry is 1:1. With 2:1 ligand:dsDNA stoichiometries, the appropriate concentration of dsDNA can be roughly approximated by taking the square root of the product of the equilibrium association constants (K_1K_2), such that $[DNA] = 1/(K_1K_2)^{1/2}$. That the concentration of dsDNA employed is appropriate must be verified visually by plotting the fluorescence signal vs $[ligand]_t$, where $[ligand]_t$ is the total concentration of ligand added to the dsDNA solution. The plot must show a significant curvature to be a usable isothermal binding curve. At higher concentrations of dsDNA, these plots effectively yield two straight lines which are useful in determining ligand:dsDNA stoichiometries but not equilibrium constants. Isothermal binding curves for dsDNA oligomers such as **1** and **12**, which contain the preferred binding site for FPH-1,

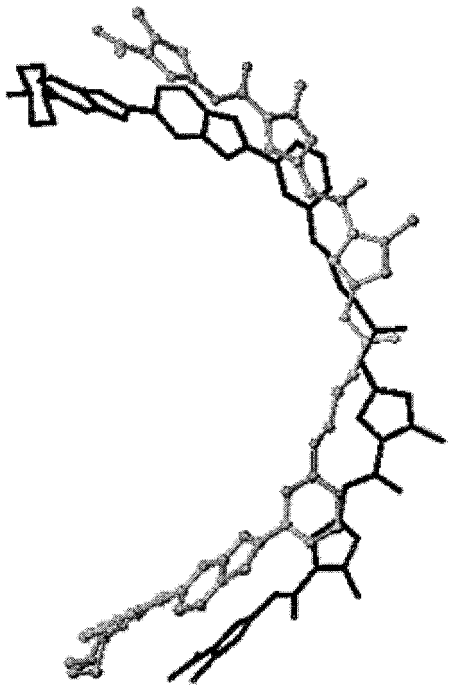

Figure 3. View down the long axis of the $(FPH\text{-}1)_2$:dsDNA complex shown in Figure 2. The dsDNA atoms are not shown in order to illustrate the curvature of the two side-by-side binding FPH-1 molecules.

were generated at dsDNA concentrations as low as 1 nM. Equilibrium constants are given as the product of K_1K_2 since separation of the individual equilibrium constants is not possible (due to their similarity in magnitude). Multiple assays gave a standard deviation of roughly ±60% for those values stated in Table 1. Titrations of the 18-mer (Table 1a) and 17-mer (Table 1b) oligomeric duplexes were accomplished in 150 and 10 mM NaCl buffers, respectively.

Stop−flow fluorimetry was accomplished using an Applied Photophysics stop−flow spectrophotometer. Samples were excited at 260 nm. Fluorescence emission was monitored by employing a 320 nm interference filter. Measurements were taken in 10 mM potassium phosphate, 10 mM NaCl, pH 7.2 buffer. Each data point shown in Figure 7 is the average of at least three trial runs. Second-order rate constants were determined as the slope through plots of k_{obs} vs [ligand] (see Figure 8a). Error values were determined by first calculating the second-order rate constants for each individual data point and then finding the standard deviation of those values from the slope of the plots of k_{obs} vs [L]. First-order off rates were determined from the *y*-intercept at [L] = 0 (Figure 8a).

Procedures (Organic Synthesis). General. ^1H and ^{13}C NMR spectra were obtained on a Varian Unity Inova 400 or 500 spectrometer at 400 MHz and 100 or 150 MHz, respectively. TLC was carried out on silica gel (KIESELGER 60 F254) glass backed commercial plates and visualized by UV light. Fast atom bombardment mass spectra, HRMS and LRMS, were obtained on a VG analytical, VG-70E double focusing mass spectrometer, with an Ion Tech Xenon Gun FAB source, and an OPUS/SIOS data interface and acquisition system. High-pressure liquid chromatography was accomplished using a Hewlett-Packard Series 1050 HPLC equipped with a diode array detector. For preparative separations an Alltech Macrosphere 300A, C8, silica, 7 μm, 250 mm × 10 mm reverse phase column was used. For analytical separations an Alltech Macrosphere 300A, C18, silica, 7 μm, 250 mm × 4.6 mm reverse phase column was used.

***tert*-Butyl 4-Nitro-1-methylpyrrole-2-carboxylate (26).** Compound **25** (1 g, 5.9 mmol) was added to 40 mL of diethyl ether and 2 mL of concentrated sulfuric acid in a round-bottom flask. The colloidal solution was cooled to −40 °C, and a steady stream of isobutylene was bubbled through the solution for several minutes. The solution was capped tightly with a rubber septa and copper wire, allowed to warm to room temperature, and stirred for 24 h. The crude reaction mixture was washed repeatedly with saturated $NaHCO_3$ and 1 M Na_2CO_3. Crude product was then further purified by flash chromatography (silica, 1:1 DCM:hexanes) to provide **26** with only minor impurities as judged by NMR (267 mg, 20% yield): TLC (1:1 DCM/hexanes) R_f 0.2; ^1H NMR ($CDCl_3$) δ 1.55 (s, 9H, $(CH_3)_3C$), 3.9 (s, 3H, CH_3-N_{Py}), 7.33 (bd, 1H, Ar H), 7.55 (m, 1H, Ar H); LREI *m*/*e* 226 ($M^{\bullet+}$ 226.23), 170, 153, 140.

***tert*-Butyl 4-Amino-1-methylpyrrole-2-carboxylate.** Without further purification **26** (230 mg, 1 mmol) was dissolved in 30 mL of methanol to which 60 mg of 10% palladium on charcoal catalyst was added. The solution was stirred underneath an atmosphere of hydrogen gas (∼1 atm) for 3 days by which time TLC (silica, DCM) showed no remaining starting material. The solution was filtered through Celite and the filtrate evaporated to give crude amine with only minor impurities and no left over starting material as judged by ^1H NMR. ^1H NMR ($CDCl_3$) δ 1.52 (s, 9H, $(CH_3)_3C$), 3.78 (s, 3H, CH_3-N_{Py}), 6.30 (d, J = 2.2 Hz, 1H, Ar H), 6.40 (d, J = 2.2 Hz, 1H, Ar H) ppm.

***tert*-Butyl 4-[(9-Fluorenylmethoxycarbonyl)amino]-1-methylpyrrole-2-carboxylate (29).** Without further purification *tert*-butyl 4-amino-1-methylpyrrole-2-carboxylate was then dissolved in 40 mL of dioxane, 20 mL of saturated $NaHCO_3$, and 5 mL of methanol to which was added FMOC-Cl (259 mg, 1 mmol). The colloidal solution was stirred at room temperature for 24 h. The product was extracted into diethyl ether and washed several times with water. The crude product was purified by flash chromatography (silica, 2.5:97.5 ethyl acetate:DCM) to provide **29** as a shiny tan/white solid (130 mg, 55% yield): TLC (2.5:97.5 ethyl acetate/DCM) R_f 0.4; ^1H NMR ($CDCl_3$) δ 1.55 (s, 9H, $(CH_3)_3C$), 3.85 (s, 3H, CH_3-N_{Py}), 4.26 (t, J = 6.59 Hz, 1H, Ph_2-CHR), 4.48 (d, J = 6.78 Hz, 2H, $-CH_2OC(=O)N-$), 6.51 (bs obscured by $CHCl_3$ absorption, $-(O=C)NH-$), 6.94 (s, 1H, pyrrole Ar H), 7.00 (s, 1H, pyrrole Ar H), 7.312 (t, J = 6.78 Hz, 2H, FMOC Ar H), 7.41 (m, 2H, FMOC Ar H), 7.61 (bd, J = 7.33 Hz, 2H, FMOC Ar H), 7.77 (d, J = 7.69 Hz, 2H, FMOC Ar H) ppm; IR (type 61 3M IR card) 2957, 2911, 1697, 1588, 1440, 1244, 1153 cm^{-1}; HRMS (FAB) 418.1886 (418.1892 calcd for $C_{25}H_{26}N_2O_4$).

Phenyl 4-Nitro-1-methylpyrrole-2-carboxylate (27). Compound **25** (2 g, 11.8 mmol), phenol (1.1 g, 11.8 mmol), and DCC (2.6 g, 12.6 mmol) were dissolved in 20 mL of DMF and stirred at room temperature for 24 h. Precipitated dicyclohexylurea was removed by filtration and solvent was then removed by evaporation under vacuum. Product was then dissolved in DCM and washed several times with saturated $NaHCO_3$. The organic layer was then dried with Na_2SO_4 before evaporation of solvent to give crude product mixture. Product was purified by flash chromatography (silica, 90:10 DCM/ethyl acetate) to provide **27** as tan powder (664 mg, 23% yield): TLC (90:10 DCM/ethyl acetate) R_f 0.30; ^1H NMR ($CDCl_3$) δ 4.04 (s, 3H, CH_3-N_{Py}), 7.17−7.2 (m, 2H, Ar H), 7.28−7.32 (m, 1H, Ar H), 7.42−7.47 (m, 2H, Ar H), 7.68−7.70 (m, 2H, Ar H); LREI *m*/*e* 246 ($M^{\bullet+}$), 153, 137, 107, 79.

Phenyl 4-[(9-Fluorenylmethoxycarbonyl)amino]-1-methylpyrrole-2-carboxylate (30). Compound **27** (134 mg, 0.54 mmol) was dissolved in 20 mL of ethyl acetate to which 30 mg of 10% palladium on carbon catalyst was added. The solution was stirred under an atmosphere of hydrogen gas (∼1 atm) for 48 h at which time, as estimated by TLC (silica, DCM/methanol), the reaction was mostly complete. The solution was filtered though Celite and evaporated to give crude product. The ^1H NMR of the crude product indicated minor impurities with very little left over starting material. TLC (100% DCM) $R_f \sim 0.00$; LREI *m*/*e* 216 ($M^{\bullet+}$ 216.23, calcd for $C_{12}H_{12}N_2O_2$), 123, 95. Without further purification the crude product was dissolved in 2 mL of saturated $NaHCO_3$ and 4 mL of dioxane to which was added FMOC-Cl (112 mg, 0.43 mmol). The colloidal reaction mixture was stirred for 24 h. Product formation was monitored by TLC (silica, 6:0.5:3.5 DCM/ethyl acetate/hexanes). The reaction mixture was diluted with diethyl ether and washed several times with water. The organic layer was then dried using Na_2SO_4 and evaporated. The crude product was then purified by flash chromatography (silica, 6:0.5:3.5 DCM/ethyl acetate/hexanes) to give **30** (124 mg, 52% yield): TLC (silica, 6:0.5:3.5 DCM/ethyl acetate/hexanes) R_f 0.55; ^1H NMR ($CDCl_3$) δ 3.90 (s, 3H, CH_3-N_{Py}), 4.29 (t, J = 6.41 Hz, 1H, Ph_2-CHR), 4.54 (d, J = 6.59 Hz, 2H, $-CH_2OC(=O)N-$), 6.74 (s, 1H, pyrrole Ar H), 6.91 (s, 1H, pyrrole Ar H), 7.17−7.19 (m Ar H), 7.23−7.28 (m obscured by $CHCl_3$ absorption, Ar H),

7.32−7.37 (m, Ar H), 7.39−7.47 (m, Ar H), 7.64 (m, 2H, FMOC Ar H) ppm, 7.80 (d, J = 7.50 Hz, 2H, FMOC Ar H) ppm; LRMS (CI/CH_4) m/e 438 ($M^{\bullet+}$).

Pentafluorophenyl 4-Nitro-1-methylpyrrole-2-carboxylate (28). Compound **25** (1 g, 5.9 mmol), pentafluorophenol (1.08 g, 5.9 mmol), and DCC (1.4 g, 5.9 mmol) were dissolved in 20 mL of DMF and stirred at room temperature for 4 h. The disappearance of compound **25** was monitored by TLC (100% DCM). The solvent was removed by evaporation under vacuum and the crude product mixture reconstituted in diethyl ether. Precipitate, including dicyclohexylurea, was removed by filtration, and the solvent was evaporated to give a sticky brown mixture. Purification was achieved by flash chromatography (silica, 1:1 DCM/hexanes) to provide **28** as a fluffy white powder (1.4 g, 71% yield): TLC (silica, 1:1 DCM/hexanes) R_f 0.4; ^{1}H NMR ($CDCl_3$) δ 4.05 (s, 3H, CH_3-N_{Py}), 7.75 (bd, 1H, pyrrole Ar H), 7.77 (m, 1H, pyrrole Ar H); ^{13}C NMR ($CDCl_3$) δ 38.297 (C-N_{Py}), 3 signals were detected in the aromatic region 115.793 + 119.799 + 129.579, 155.950 (Py-C(=O)−) ppm; IR (type 61 3M IR card) 3140, 2918, 2847, 1758, 1519, 1322, 1042 cm^{-1}; LRMS (FAB) 336 (M + H)$^+$.

Pentafluorophenyl 4-[(9-Fluorenylmethoxycarbonyl)amino]-1-methylpyrrole-2-carboxylate (31). Compound **28** (700 mg, 2.1 mmol) was dissolved in 100 mL of 1:1 ethyl acetate/ethanol. To this solution was added 2 mL of saturated $NaHCO_3$ and 80 mg of 10% palladium on carbon catalyst. The solution was stirred under an atmosphere of hydrogen gas (∼1 atm) for 48 h. Reaction progress was monitored by TLC. The solution was filtered through Celite and the filtrate reduced to a volume of ∼10 to 20 mL. The reduced filtrate was combined with 25 mL of dioxane, an additional 5 mL of saturated $NaHCO_3$, and FMOC-Cl (596 mg, 2.2 mmol). The solution was stirred for 16 h at room temperature. Product was extracted into diethyl ether and the organic layer washed several times with water. Product was purified by flash chromatography (silica, 4:6:0.5 DCM/hexanes/ethyl acetate) to give **31** as a shiny white powder (837 mg, 75% yield). TLC (silica, 4:6:0.5 DCM/hexanes/ethyl acetate) R_f 0.2; ^{1}H NMR ($CDCl_3$) δ 3.90 (s, 3H, CH_3-N_{Py}), 4.27 (t, J = 6.41 Hz, 1H, Ph_2-CHR), 4.53 (d, J = 6.59 Hz, 2H, −CH_2OC(=O)N−), 6.56 (s, 1H, pyrrole Ar H), 6.96 (s, 1H, pyrrole Ar H), 7.27 (bs obscured by $CHCl_3$ absorption, −(O=C)-NH−), 7.33 (m, 2H, FMOC Ar H), 7.42 (t, J = 7.51 Hz, 2H, FMOC Ar H), 7.61 (bd, J = 7.50 Hz, 2H, FMOC Ar H), 7.78 (d, J = 7.51 Hz, 2H, FMOC Ar H) ppm; ^{13}C NMR ($CDCl_3$) δ 37.06 (C-N_{Py}), 47.33 (−COC(=O)N−), 67.23 (−CCOC(=O)N, the following 10 signals were detected in the aromatic region 110.775 + 116.784, 120.266 + 122.739 + 123.088 + 125.106 + 127.337 + 128.027 + 141.562 + 143.868, 153.898 (−C(=O)N−), 156.348 (Py-C(=O)−) ppm; IR (type 61 3M IR card) 2920, 1743, 1589, 1520, 1448, 1221, 1032, 742 cm^{-1}; HRMS (FAB) 528.1105 (528.1108 calcd for $C_{27}H_{17}N_2O_4F_5$).

FPH-1. The solid-phase synthesis of FPH-1 was accomplished using MBHA rink amide resin (53 mg, 0.0265 mmol loading sites) and standard manual solid-phase FMOC techniques. Coupling reactions were accomplished using 2.5 equiv of **31**, 2 equiv of HOBt, and 4 equiv of DIPEA in anhydrous DMF and were run for 24 h. High coupling yields between 70 and 100% were measured by absorption at 290 nm of deprotected FMOC after resin was treated with a 20% piperidine/DMF solution. Coupling of **34** to the growing polyamide chain was accomplished using 2.5 equiv of **34**, 2.5 equiv of PyBOP, and 8 equiv of DIPEA for 24 h. Resin cleavage was achieved in 4 h using a 95% TFA, 2.5% water, and 2.5% TIS solution. Product was purified by HPLC with an increasing gradient of acetonitrile in 0.1% aqueous TFA solution. After purification the product was precipitated out of a methanol/ether solution with anhydrous HCl gas. Product purity was shown by analytical HPLC. Yield was determined by NMR spectroscopy (as mentioned above) to be 3.0×10^{-6} mol (11% yield): ^{1}H NMR ($CDCl_3$) δ 2.12 (m, 2H, −CH_2COPh), 2.5 (overlapped by DMSO solvent peak, −CH_2OPh), 2.90 (s, 3H, CH_3-NR_2), 3.82 (s, overlaps HOD absorption, CH_3-N_{Py}), 3.85 (s, overlaps HOD absorption, CH_3-N_{Py}), piperazine ring CH_2 signals are hidden by HOD absorption, 4.18 (t, overlaps HOD absorption, J = 5.74 Hz, NC(=O)CH_2−), signals detected between 7 and 9 ppm are due to Ar H and carbamate protons, 7.15 (m) + 7.23 (m) + 7.53 (bt) + 7.66 (m) + 7.85 (s) + 8.11 (m) + 8.52 (s) ppm; LRMS (FAB) 878 (M + H)$^{+1}$. Fluorescence emission spectrum: broad peak centered at 475 nm. UV spectrum: λ(max) = 318 nm, λ(min) = 284 nm (FPH-1 was observed to obey the Beer−Lambert law at μM concentrations in contrast to Hoechst 33258 which does not[27]).

Results

The synthesis of FPH-1 was accomplished in a stepwise manner from MBHA rink amide resin by employing FMOC chemistry and standard manual solid-phase synthetic techniques (Scheme 1).[28] It should be noted that the synthesis of **32** and its use in the solid-phase synthesis of a polyamide has been previously communicated.[29] However, we were unable to synthesize the FMOC-protected monomer **32** via the reported catalytic hydrogenation of **25**. Esterified products **26** and **27**, unlike **25**, were found to reduce cleanly by catalytic hydrogenation. Amino pyrroles are well known for their instability, making it difficult to purify them.[30] The unpurified amines of **26** and **27** were protected with FMOC-Cl, giving **29** and **30**. Unfortunately, it was not possible to hydrolyze either molecule. The FMOC protecting group was not stable to the harsh conditions needed to hydrolyze **30**. Deprotection of **30** with hydrogen peroxide was also unsuccessful.[31] The *tert*-butyl esters of pyrrole carboxylates such as **26** and **29** are sometimes easily removed by trifluoroacetic acid.[30,32] However, deprotection of **29** occurred only in concentrated sulfuric acid and in extremely low yields due to decomposition of starting material or possibly decarboxylation of the product. Pyrrole carboxylic acids are known to readily decarboxylate when heated.[30,33] Pentafluorphenyl esters are widely used in the solid-phase synthesis of peptides; still the pentafluorphenyl pyrrole carboxylate **28** was found to be fairly stable, reducing cleanly without any traces of hydrolysis or polymerization.[34] Coupling of **31** to the primary amine of the MBHA rink amide resin proceeded very slowly, giving onlya 10% yield after 24 h. Yields were increased greatly by the addition of HOBt. Coupling reactions were monitored by the UV absorption of the deprotected FMOC. The traditional Kaiser test is not compatible with the aromatic amine of the pyrrole ring.[35] Coupling yields between pyrrole units were observed to be between 80 and 100%.

Ligand:dsDNA complex stoichiometries were determined by spectrofluorometric titration.[25] Similar to Hoechst 33258, the fluorescence emission of FPH-1 also increases greatly upon complexation of dsDNA. Upon excitation at 345 nm, FPH-1:dsDNA complexes emit a broad fluorescence signal centered at 470 nm, red shifted ∼20 nm with respect to Hoechst 33258. Generally Hoechst 33258:dsDNA complexes are excited near 350 nm and emit a broad fluorescence signal centered at 450 nm.[26,27,37−40] All of the oligomeric duplexes investigated (Table

(27) Loontiens, F. G.; Regenfuss, P.; Zechel, A.; Dumortier, L.; Clegg, R. M. *Biochemistry* **1990**, *29*, 9029−9039.
(28) Fields, G. B.; Noble, R. L. *Int. J. Pept. Protein Res.* **1990**, *35*, 161−214.
(29) Vazquez, E.; Caamano, A. M.; Castedo, L.; Mascarenas, J. L. *Tetrahedron Lett.* **1999**, *40*, 3621−3624.
(30) Jones, R. A. *Pyrroles*; John Wiley and Sons, Inc.: New York, 1992; Vol. 48, pp 315−316.
(31) Kenner, G. W.; Seely, J. H. *J. Am. Chem. Soc.* **1971**, *94*, 3259−3260.
(32) Crook, P. J.; Jackson, A. H.; Kenner, G. W. *J. Chem. Soc. C* **1971**, 474−487.
(33) Joule, J. A.; Mills, K.; Smith, G. F. *Heterocyclic Chemistry*, 3rd ed.; Chapman and Hall: London, 1995; pp 244−245.
(34) Kisfaludy, L.; Schon, I. *Synthesis* **1983**, 325−327.
(35) Sarin, V. K.; Kent, S. B. H.; Tam, J. P.; Merrifield, R. B. *Anal. Biochem.* **1981**, *117*, 147−157.
(36) Chadwick, D. J.; Chambers, J.; Meakins, D. G.; Snowden, R. L. *J. Chem. Soc., Perkin Trans. I* **1973**, 1766−1773.
(37) He, G. X.; Browne, K. A.; Blasko, A.; Bruice, T. C. *J. Am. Chem. Soc.* **1994**, *116*, 3716−3725.

Scheme 1

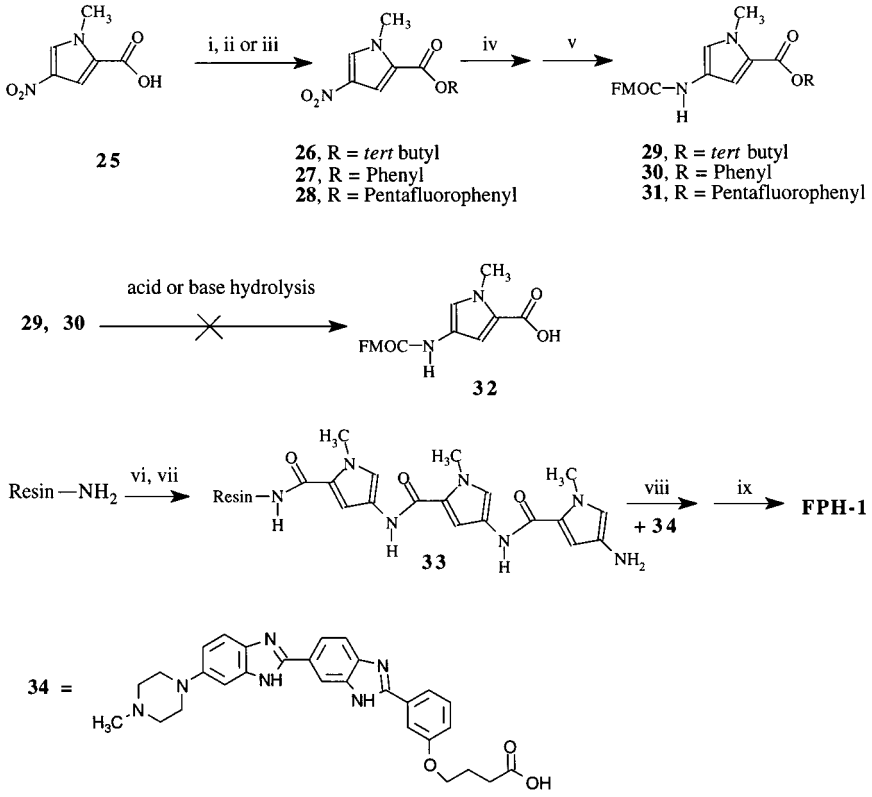

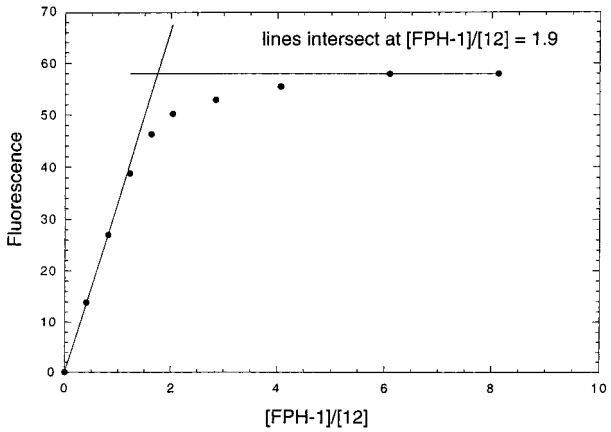

Figure 4. Titration of 33 μM **12** with FPH-1. Plots shows relative fluorescence intensity at 475 nm in arbitrary units vs ligand:DNA ratio. The two straight lines were generated by linear least squares fitting of data points early and late in the titration. The point of intersection of the two lines over the *x*-axis provides the stoichiometry of the ligand:DNA complex.

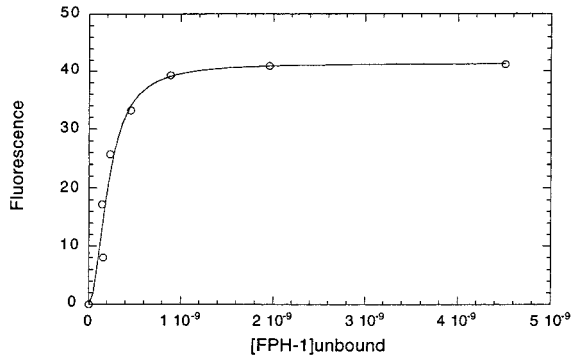

Figure 5. Isothermal binding curve generated by spectrofluorometric titration of 3 nM **12** with FPH-1. Plots show relative fluorescence intensity in arbitrary units vs concentration unbound FPH-1 as calculated by eq 2. Data points were fit using eq 1.

1) were determined to form $(FPH\text{-}1)_2$:dsDNA complexes. Additionally, all oligomeric duplexes whose equilibrium association constants for complexation by Hoechst 33258 are listed in Table 1 were also found to form $(Ht33258)_2$:dsDNA complexes. In contrast, the oligomeric duplex **23** was determined to form a Ht33258:**23** complex with a 1:1 stoichiometry (no equilibrium association constant is given in Table 1 for the Ht33258:**23** complex). Figure 4 shows a representative example of a plot used to determine FPH-1:dsDNA stoichiometry.

Equilibrium association constants for complexation of dsDNA were determined via spectrofluorometric titrations (see Table 1 and Figure 5). FPH-1 is highly selective for its nine base pair target site, whereas Hoechst 33258 shows no such selectivity. For example, whereas equilibrium association constants (K_1K_2) for formation of Hoechst 33258 complexes with **1** and **11** are nearly equal (oligomers **1** and **11** both contain two separate and nonoverlapping binding sites for Hoechst 33258), the equilibrium constants for formation of FPH-1 complexes with **1** and **11** differ by greater than 4 orders of magnitude. The same is true for oligomers **12** and **22** whose equilibrium constants for complexation by Hoechst 33258 are again nearly equal while those for complexation of **12** and **22** by FPH-1 differ by 9000-fold (oligomers **11** and **22** both contain double base pair mismatches). Similar comparison of equilibrium constants for single base pair mismatch oligomers **6** and **17** also demonstrate the selectivity of FPH-1. All single base pair mismatches of oligomers **1** and **12** cause significant decreases in K_1K_2 ranging from 18- to 2300-fold.

(38) Bostock-Smith, C. E.; Searle, M. S. *Nucl. Acids Res.* **1999**, *27*, 1619−1624.
(39) Haq, I.; Ladbury, J. E.; Chowdhry, B. Z.; Jenkins, T. C.; Chaires, J. B. *J. Mol. Biol.* **1997**, *271*, 244−257.
(40) Loontiens, F. G.; McLaughlin, L. W.; Diekmann, S.; Clegg, R. M. *Biochemistry* **1991**, *30*, 182−189.

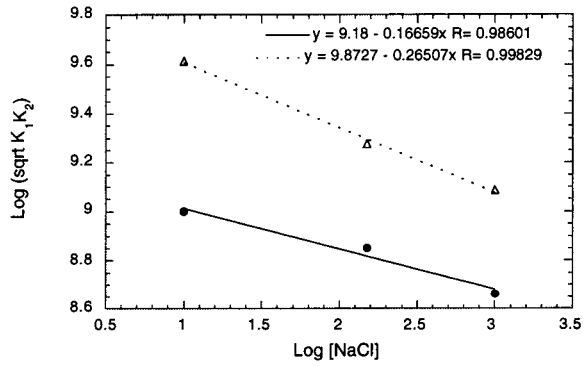

Figure 6. Ionic strength dependence of the equilibrium constants for association of FPH-1 (△) and Hoechst 33258 (○) with oligomeric duplex **1**.

Table 2. Melting Temperatures for Ligand:DNA Complexes (°C)[a]

DNA oligomers	t^0_m	Δt_m FPH-1	Δt_m Ht33258
5′-GCGGTATAAAATTCGACG-3′ (**1**)	60	10	5
5′-GCGG**C**ATAAAATTCGACG-3′ (**2**)	63	6	3
5′-GCGG**T**GTAAAATTCGACG-3′ (**3**)	62	4	3
5′-GCGGTA**C**AAAATTCGACG-3′ (**4**)	61	4	3
5′-GCGGTAT**G**AAATTCGACG-3′ (**5**)	62	2	3
5′-GCGGTATA**G**AATTCGACG-3′ (**6**)	61	1	2
5′-GCGGTATAA**G**ATTCGACG-3′ (**7**)	60	3	2
5′-GCGGTATAAA**G**TTCGACG-3′ (**8**)	61	2	2
5′-GCGGTATAAAA**C**TCGACG-3′ (**9**)	62	2	2
5′-GCGGTATAAAAT**C**CGACG-3′ (**10**)	61	6	2
5′-GCGGTATA**GG**AATTCGCG-3′ (**11**)	60	0	3
5′-GCGAATTTAATTCGACG-3′ (**12**)	58	13	6
5′-GCGAATT**CC**AATTGACG-3′ (**22**)	59	1	3

[a] t_m values for oligomer complexes were determined by first derivative analysis. t^0_m are melting temperatures of oligomeric duplexes in pH 7 buffer containing 150 mM NaCl in the absence of ligand. Δt_m are differences in melting temperatures for oligomeric duplexes in the absence and presence of ligand. Standard deviation for Δt_m values are ±1 °C.

The ionic strength dependence of the equilibrium constant for association of FPH-1 with the oligomeric duplex **1** was investigated. Figure 6 shows plots of log $(K_1K_2)^{1/2}$ vs log [NaCl] for both FPH-1 and Hoechst 33258. The affinity of both ligands for **1** decreases with ionic strength: $\partial \log (K_1K_2)^{1/2}/\partial \log$ [NaCl] are −0.2 and −0.3 for FPH-1 and Hoecsht 33258, respectively. The log of the *square root* of K_1K_2 is plotted vs log [NaCl] because the resulting slope is unitless. In constrast, a plot of log K_1K_2 vs log [NaCl] results in a slope with units M^{-1}. A unitless slope is needed to be able to compare our values with those previously reported for Hoechst 33258 from plots of $\partial \log K/\partial \log$ [NaCl].[27]

The thermal stability of $(FPH\text{-}1)_2$:dsDNA complexes were investigated by thermal denaturation experiments. As shown in Table 2, FPH-1 forms significantly more stable complexes with oligomers **1** and **12** than does Hoechst 33258 (Figure 7). The effect of FPH-1 on Δt_m (the difference between t_m values for oligomeric duplexes in the absence and presence of ligand) decreases greatly for oligomers **2**−**10** which all contain single base pair mismatches. Δt_m values tend to be more stronglyaffected when the base pair mismatch does not reside at either end of the FPH-1 binding site. FPH-1 had almost no effect on t_m for many of the oligomers listed in Table 2 which indicates that it binds oligomeric duplexes which contain base pair mismatches weakly. For instance, oligomer **6** which contains a single base pair mismatch has a Δt_m value of only 1 °C. Oligomers **11** and **22** contain double base pair mismatches and also have Δt_m values of only 0 and 1 °C, respectively. Hoechst 33258 raises the t_m for all the oligomers investigated by 2−6 °C.

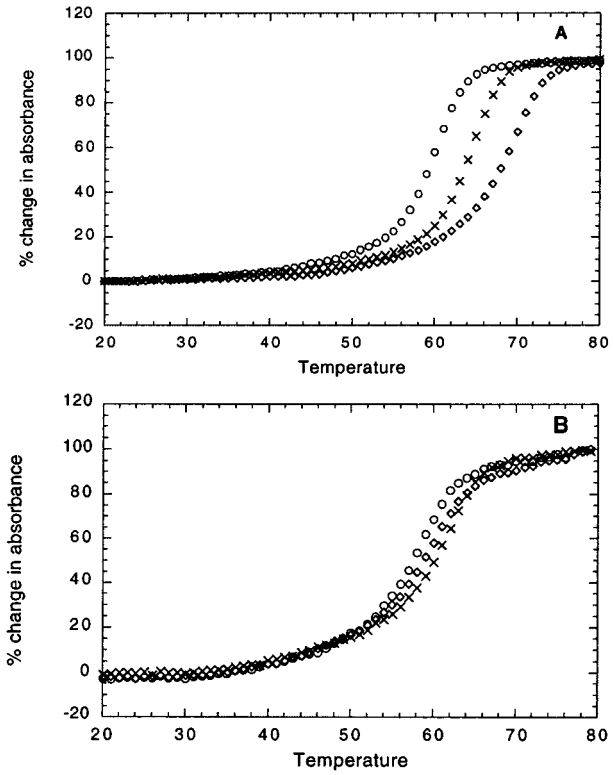

Figure 7. Thermal melting curves for oligomers **1** (0.28 μM, panel A) and **11** (0.37 μM, panel B) and their ligand (2 equiv) complexes: DNA + FPH-1 (◊), DNA + Hoechst 33258 (×), and DNA with no ligand (○).

Kinetics for the formation of FPH-1 and Hoechst 33258:**12** complexes were investigated by stop−flow fluorimetry.[41] The reactions were determined to be first order with respect to [L] and [**12**]. Reaction order was determined by plotting pseudo-first-order rate constants (excess ligand) vs [L] or [DNA] as shown in Figure 8. The second-order rate constants were determined to be $6 \pm 2 \times 10^7$ and $5 \pm 2 \times 10^8$ s^{-1} M^{-1} for FPH-1 and Hoechst 33258, respectively, indicating complexation of **12** at near diffusion controlled and diffusion controlled rates, respectively. The first-order off rates were determined to be <1 and 20 s^{-1} for FPH-1 and Hoechst 33258, respectively.

Discussion

We sought to design a minor groove binding agent which would recognize an extended sequence of base pairs and have ready entrance to cells and the nucleus. The design of FPH-1 allows for easy observation of invivo and invitro reactions with dsDNA by fluorescence spectroscopy. The biological activity of FPH-1 is currently under investigation including the use of fluorescence microscopy to investigate cellular localization and uptake (fluorescence microscopy has been previously employed to show the selective localization in nuclear DNA of certain bis-bezimidazole type compounds[42]). Spectrofluorometric titrations were employed to investigate stoichiometries and equilibrium constants for formation of FPH-1:dsDNA complexes. The technical benefit gained by employing a molecule which

(41) Baliga, R.; Crothers, D. M. *Proc. Natl. Acad. Sci. U.S.A.* **2000**, *97*, 7814−7818.

(42) Harapanhalli, R. S.; Howell, R. W.; Rao, D. V. *Nucl. Med. Biol.* **1994**, *21*, 641−647.

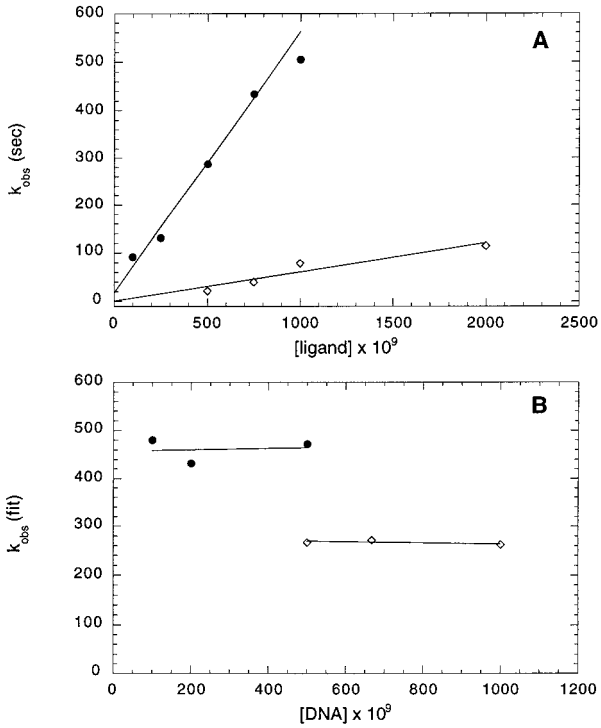

Figure 8. Plots of pseudo-first-order rate constants for complexation of DNA by excess ligand determined via stopped-flow fluorimetry. Panel A: addition of excess Hoechst 33258 (●) or FPH-1 (◊) to 100 or 500 nm **9**, respectively. Panel B: addition of 1000 nM Hoechst 33258 (●) or 3000 nM FPH-1 (◊) to varying concentrations of **9**.

fluoresces upon binding dsDNA is shown by the long list of oligomeric duplexes we have been able to investigate (Table 1). In contrast, literature reports of nonfluorescent minor groove binders are often limited to investigation of one or two dsDNA binding sites which make it difficult to asses details of sequence specificity.[10−16,18,19]

All of the oligomeric duplexes investigated (Table 1) were determined to form $(FPH\text{-}1)_2$:dsDNA complexes. Additionally, all oligomeric duplexes whose equilibrium association constants for complexation by Hoechst 33258 are listed in Table 1 were also found to form $(Ht33258)_2$:dsDNA complexes. The structures of the $(FPH\text{-}1)_2$:dsDNA and $(Ht33258)_2$:dsDNA complexes are quite different. The observed 2:1 FPH-1:dsDNA complex stoichiometries suggest the formation of side-by-side trimeric complexes as depicted in Figure 2. This will be discussed later. Consistent with known characteristics, each Hoechst 33258 molecule in a $(Ht33258)_2$:dsDNA complex resides in a four dA/dT base pair region such that the two Hoechst molecules are arranged end-to-end and do not overlap each other.[43,44] The stoichiometry of Ht33258:dsDNA complexes depends on the number of Hoechst 33258 binding sites contained within the dsDNA oligomer. For example, the oligomeric duplex **17** which contains two Hoechst 33258 binding sites separated by a G/C base pair d(-AATTCAATT-) forms a $(Ht33258)_2$:**17** complex. The oligomeric duplex **23** contains a single Hoechst 33258 binding site of d(-AATT-) and forms only the 1:1 Ht33258:**23** complex.

Equilibrium association constants were determined for complexation of 35 different oligomeric duplexes by FPH-1 (Table 1). As shown in Table 1, FPH-1 is clearly selective for its preferred nine dA/dT base pair binding site as contained within oligomers **1** and **12**. Generally, the negative effect of single base pair mismatches on K_1K_2 is greater when the position of the mismatched base pair resides in the center of the FPH-1 binding site. Comparison of equilibrium constants, K_1K_2, listed in Table 1 shows that the overall effect of a base pair mismatch is equivalent for oligomers **1** and **12**. As shown in Table 1 FPH-1 shows a very slight preference (∼5-fold) for oligomer **12** over **1** but overall shows no general ability to differentiate between two different A/T rich binding sites. The few K_1K_2 values determined for Hoechst 33258 are similar in magnitude (within a factor of 10). Hoechst 33258 shows no selectivity for longer DNA binding sites. Additionally, K_1K_2 values for FPH-1 complexes with **1** and **12** are significantly greater than for their respective Hoechst 33258 complexes (by factors of 10- and 70-fold, respectively).

The ionic strength dependence of the equilibrium constants for association of FPH-1 and Hoechst 33258 with **1** are roughly equivalent with slopes of −0.3 and −0.2, respectively (see Figure 6). The effect of increasing NaCl concentrations by a factor of 10 is calculated to decrease K_1K_2 values by a factor of 2 to 3 for either ligand. The ionic strength dependence of the equilibrium constant for association of Hoecsht 33258 with poly[d(A-T)] has been previously reported to be $\partial \log K/\partial \log [NaCl] = -0.76$.[27] This indicates that the ionic strength dependence of the equilibrium constant for assocation of Hoecsht 33258 with DNA appears to vary significantly depending upon the type of DNA being investigated.

Thermal denaturation experiments were employed as an alternative method for investigation of FPH-1 sequence selectivity. As indicated in Table 2, FPH-1 selectively stabilizes oligomeric duplexes which contain a nine base pair A/T rich binding site. Parallel to decreases in K_1K_2 values, single base pair mismatches within the FPH-1 binding site cause large decreases in Δt_m values. For instance, oligomer **6** contains a single base pair mismatch and has a Δt_m value of only 1 °C. Additionally, oligomers **11** and **22** contain double base pair mismatches and have Δt_m values of only 0 and 1 °C, respectively. In contrast, Hoechst 33258 Δt_m values are fairly similar for all the oligomers investigated. Thus, as measured by differences in K_1K_2 and in Δt_m values, FPH-1 is able to distinguish between oligomeric duplexes indistinguishable by Hoechst 33258.

Hoechst 33258 is not long enough to recognize sequences of more than four DNA base pairs. Attempts to target longer sequences have been made by synthesizing longer molecules with a larger number of benzimidazole or pyrrole units.[15,45] However, the curvature of these extended molecules fails to match the natural curvature of the minor groove of DNA. This problem was overcome by employing polyamide-type molecules connected with linkers.[11] These types of molecules are capable of forming highly stable DNA complexes. Interestingly, many of these long polyamides were never investigated for their sequence selectivity beyond qualitative footprinting experiments from which the authors simply concluded that these long molecules bound both short and long A/T rich tracts. In other cases, the molecules formed strong DNA complexes but showed a lack of sequence selectivity.[10,14]

Experimental results rule out the possibility of hairpin[46] formation. A FPH-1 hairpin would be expected to have a binding site of four to five base pairs, similar to Hoechst 33258 or a

(43) Neidle, S. *Biopolymers* **1997**, *44*, 105−121.
(44) Geierstanger, B. H.; Wemmer, D. E. *Annu. Rev. Biophys. Biomol. Struct.* **1995**, *24*, 463−493.
(45) Pilch, D. S.; Xu, Z. T.; Sun, Q.; LaVoie, E. J.; Liu, L. F.; Breslauer, K. J. *Proc. Natl. Acad. Sci. U.S.A.* **1997**, *94*, 13565−13570.
(46) de Clairac, R. P. L.; Seel, C. J.; Geierstanger, B. H.; Mrksich, M.; Baird, E. E.; Dervan, P. B.; Wemmer, D. E. *J. Am. Chem. Soc.* **1999**, *121*, 2956−2964.

tripyrrole polyamide. For example, an oligomeric duplex such as **5** (which contains the binding site 5′-AAATT-3′) would be expected to form a highly stable FPH-1:**5** hairpin-type complex. Investigations instead show formation of an relatively weak (FPH-1)$_2$:**5** complex ($\Delta t_m = 2$ °C, $K_1K_2 = 2.1 \times 10^{17}$). Basic model building suggests that a FPH-1 hairpin (where the tripyrrole moiety folds back over the bis-benzimidazole rings) does not form due to steric clashes between the terminal pyrrole unit and the bulky piperizine ring (this same steric clash is avoided in the side-by-side antiparallel (FPH-1)$_2$:dsDNA complex shown in Figure 2 because the two FPH-1 molecules are staggered).

The ability of FPH-1 to conform to the curvature of the minor groove of DNA is shown in the side-by-side antiparallel (FPH-1)$_2$:dsDNA complex of Figures 2 and 3. The structure in Figures 2 and 3 were generated via a molecular modeling program and illustrate the curvature of the two FPH-1 molecules when placed in a side-by-side manner within the minor groove. The antiparallel side-by-side complex of FPH-1 with dsDNA has precedence since monocationic minor groove binders have a propensity to complex dsDNA in this manner.[2,21,22,47] Previous investigations show that bis-benzimidazole compounds related to **34** (Scheme 1) form side-by-side complexes with dsDNA[25] even though Hoechst 33258 does not. Placing the bis-benzimidazole moiety of one FPH-1 molecule adjacent to the tripyrrole moiety of the second FPH-1 molecule in an antiparallel arrangement avoids placement of the bulky and positively charged piperizine rings against one another. Also, slightly staggering the two FPH-1 molecules avoids placing the terminal primary amide of one FPH-1 molecule adjacent to the bulky piperazine ring of the other. Staggering the molecules is especially reasonable since structural investigations of side-by-side complexes of polyamides with dsDNA consistently showthe two polyamide molecules of the trimeric complex to be both antiparallel and staggered.[2,21,22,47]

Rate constants were determined for complexation of **12** by FPH-1 and Hoechst 33258. The rate constant for formation of the Hoechst 33258:**12** complex is diffusion-controlled. This result is consistent with literature reports that distamycin also complexes DNA at diffusion-controlled rates.[41] The rate constant for complexation of **12** by FPH-1 is somewhat slower (6×10^7 M^{-1} s^{-1}) although still near diffusion controlled.

Acknowledgment. This work was supported by a grant from the National Institute of Health (5R37DK09171-36).

JA003095D

(47) Kielkopf, C. L.; Baird, E. E.; Dervan, P. B.; Rees, D. C. *Nat. Struct. Biol.* **1998**, *5*, 104−9.